Int J Adv Manuf Technol (2015) 76:1865–1877
DOI 10.1007/s00170-014-6370-x

ORIGINAL ARTICLE

Planetary motion combined with two-dimensional vibration-assisted magnetic abrasive finishing

Yi-Hsun Lee · Kun-Ling Wu · Chung-Ting Bai · Chen-Yuan Liao · Biing-Hwa Yan

Received: 17 February 2014 / Accepted: 8 September 2014 / Published online: 27 September 2014

Abstract This study develops a new surface polishing approach by combining planetary motion (PM) with two-dimensional vibration-assisted magnetic abrasive finishing (PM-2DVAMAF). Planetary motion involves both rotation and revolution, thus generating radial acceleration, which strengthens the normal force exerted on the workpiece surface, and in turn enhances the cutting power of the abrasives and their polishing performance. Assisted by two-dimensional vibration, PM results in uniform, intersecting, and closely packed polishing paths, which contribute to better surface quality within a shorter processing time. This study also uses the Taguchi experimental design method to obtain the optimal combination of PM-2DVAMAF parameters for surface roughness improvement. The optimal combination obtained includes working gap, 1 mm; amplitude of vibration, 0.1 mm; particle size of steel grit, 0.125 mm; weight of SiC, 3 g; weight of steel particles, 0.5 g; weight of machining fluid, 5 g; frequency of vibration along the *X*- and *Y*-directions, 16.67 Hz; and rotational speed of magnet, 500 rpm. Experimental results reveal that 12.5-min PM-2DVAMAF under optimal combination of parameters can reduce surface roughness of a stainless steel SUS304 workpiece from 0.14 to 0.032 μm, an improvement rate of 77.1 %. PM-2DVAMAF can indeed improve surface quality with a short machining time and less abrasives required, both of which contribute to cost reduction and more environmentally friendly machining method in industry.

Y.-H. Lee · C.-T. Bai · C.-Y. Liao · B.-H. Yan (✉)
Department of Mechanical Engineering, National Central University, No. 300, Jhongda Rd., Taoyuan County, Jhongli City 32001, Taiwan, Republic of China
e-mail: bhyen@cc.ncu.edu.tw

K.-L. Wu
Department of Mechanical Engineering, Tungnan University, New Taipei City, Taiwan

Keywords Planetary motion combined with two-dimensional vibration-assisted magnetic abrasive finishing (PM-2DVAMAF) · Two-dimensional vibration-assisted MAF (2D VAMAF) · Magnetic abrasive finishing (MAF) · Vibration assistance · Stainless steel · Surface roughness

1 Introduction

With rapid advances in technology, electronics industries have strived to produce multifunction portable devices which are thin and compact, thus increasing the demand for components even smaller in size but with greater precision. To meet these requirements, the mold and process for fabricating such components should not only have minimum dimensional, shape, and positional tolerance but also small surface roughness. However, miniature components pose challenges to traditional polishing approaches, not to mention the extra difficulty incurred by curved or uneven surface.

Magnetic abrasive finishing (MAF), which features self-sharpening capability, self-adaptability, and self-controllability, is an ideal polishing approach for flat, curved, or uneven surface [1–4]. In addition, it can also perform deburring of metallic recast layer. MAF involves unidirectional polishing of surface, during which the gap between the workpiece and the magnet is filled with ferromagnetic particles and the grinding pressure is controlled by a magnetic field. Under the magnetic field, the abrasives will gather to form a flexible magnetic brush which does not require dressing. Thus, the magnetic abrasives can move and slide along the profile of a complex surface to perform polishing, making it superior to conventional surface-finishing approaches.

Several studies had reported a close correlation between polishing quality obtained by MAF under vibration assistance and the mode of vibration [5–7]. Two-dimensional vibration-assisted MAF (2D VAMAF), which involves simultaneous

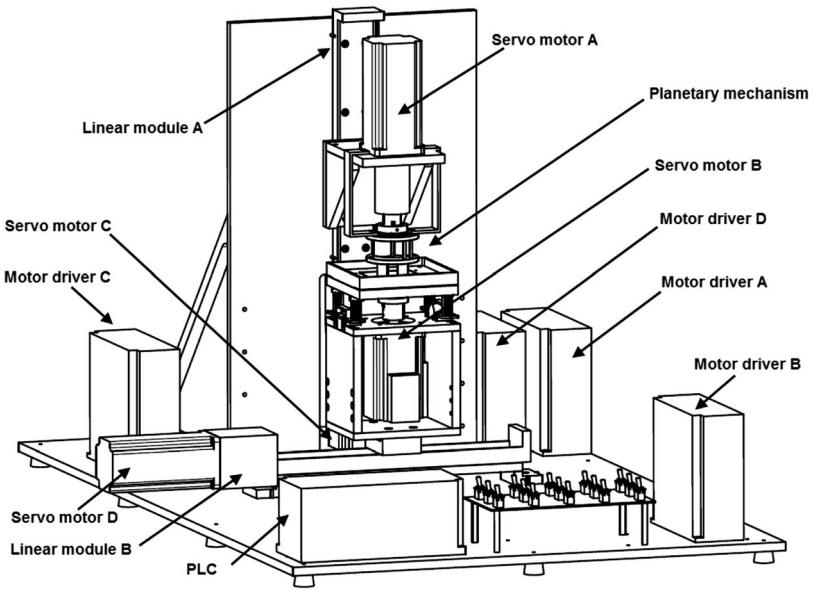

(a)

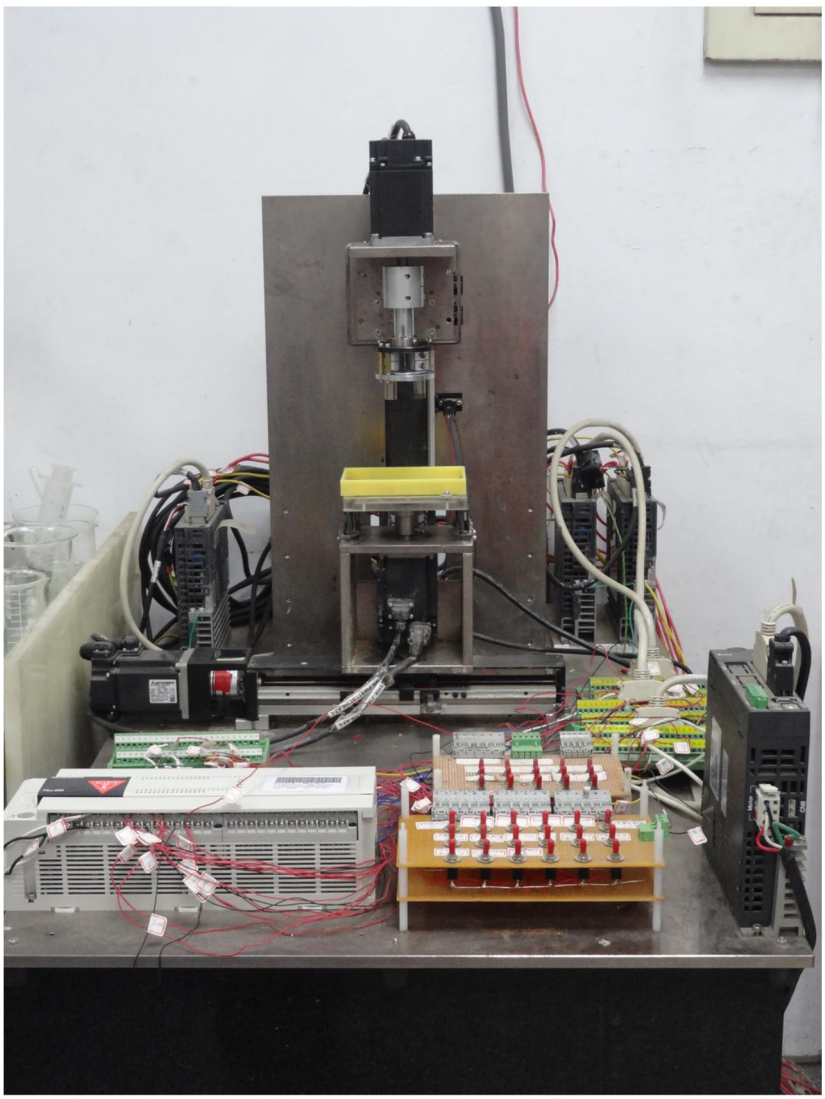

(b)

Fig. 1 **a** Schematic diagram and **b** actual photograph of PM-2DVAMAF platform

vibration in both the *X*-axis and *Y*-axis, has been found to overcome the drawback of deep scratches formed by MAF with horizontal vibration on the *X*-axis or *Y*-axis alone. Not only can 2D VAMAF enhance surface quality, it can also help improve machining efficiency and reduce machining time required. Experimental research has found an improvement in surface roughness of 77 % achieved by 5-min 2D VAMAF under optimal combination of parameters [8].

The literature contains plentiful studies on MAF with and without vibration assistance and its applications. To name a few, Mulik and Pandey [9, 10] integrated ultrasonic vibrations with MAF (UAMAF) to process AISI 52100 steel surfaces and obtained improved surface quality within a shorter processing time. Yin and Shinmura [11] applied vertical vibration-assisted MAF to deburring magnesium alloy and achieved more efficient material removal compared with deburring of brass and stainless steel. Wang and Hu [12] performed inner surface finishing of tubing made of Ly12 aluminum alloy, 316L stainless steel, and H62 brass by MAF and successfully reduced surface roughness from 9.6 to 0.24 μm. Jain et al. [13] studied the effect of working gap and circumferential speed on the material removal rate (MRR) and surface roughness. Their findings reveal that the larger the working gap and the slower the circumferential speed, the poorer the MRR is, and the faster the circumferential speed, the better is the surface quality achieved. Hung et al. [14] used MAF to process cylindrical tube of stainless steel SUS304 and explored the processing characteristics and the prediction system. They found that spindle speed, vibration frequency, discharge current, and abrasive weight ratio have a significant influence on surface roughness and the prediction system developed could attain 97 % accuracy.

In this study, PM was combined with 2D VAMAF (PM-2DVAMAF) to polish stainless steel surface. Planetary motion involves both rotation and revolution, thus generating radial acceleration, which strengthens the normal force exerted on the workpiece surface, and in turn enhances the cutting power of the abrasives and their polishing performance. Assisted by 2D vibration, PM results in uniform, intersecting, and closely packed polishing paths, which contribute to better surface quality within a shorter processing time. Moreover, PM coupled with 2D vibration can ensure smooth motion and sliding of non-sintered magnetic abrasives comprising steel particles mixed with SiC, thus preventing collision of abrasives and scratches formed on workpiece surface.

Experimental results show that PM-2DVAMAF is superior to traditional MAF and 2D VAMAF. Not only can it improve surface quality, a shorter processing time and a smaller amount of abrasives are also required, both of which contribute to cost reduction. Moreover, being an ultraprecision machining technique, PM-2DVAMAF also has the advantage of requiring structurally safe, compact, and lightweight machining equipment whose smooth running incurs less noise.

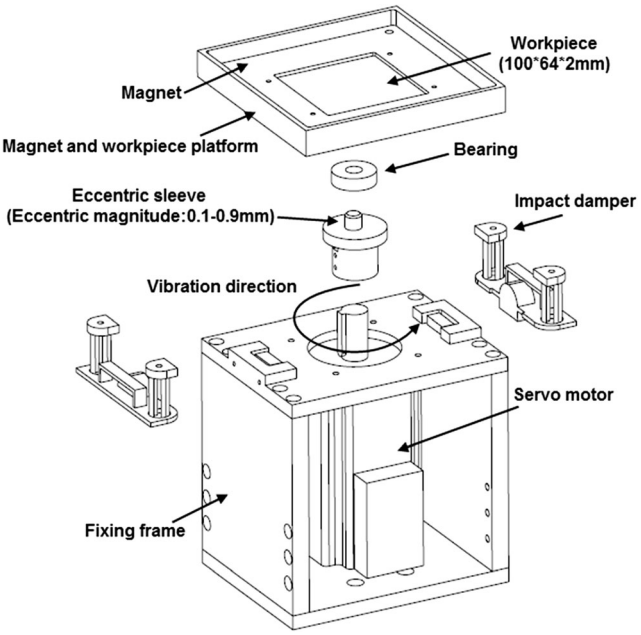

Fig. 2 Exploded view of vibration assistance mechanism

2 Experimental design

2.1 Experimental setup

Figure 1 shows the schematic diagram and actual photograph of the self-developed PM-2DVAMAF platform. As can be

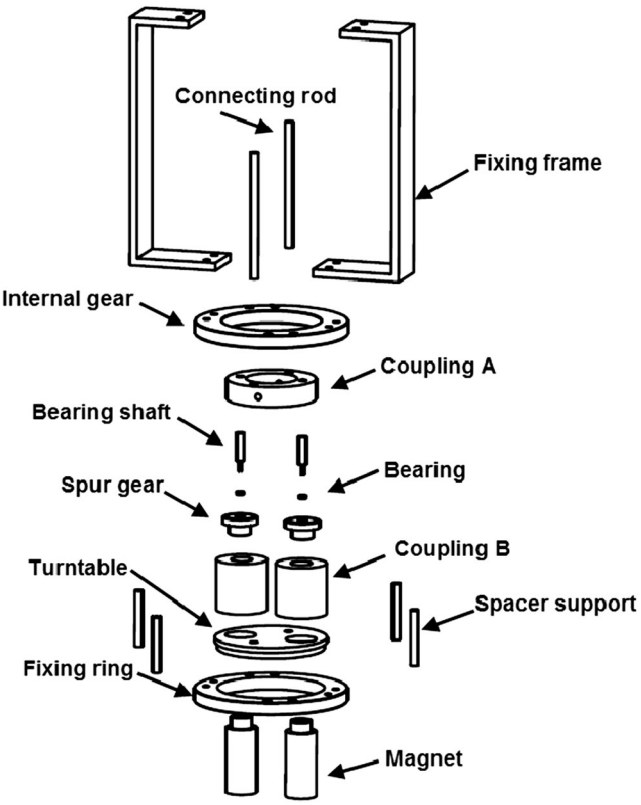

Fig. 3 Exploded view of planetary motion mechanism

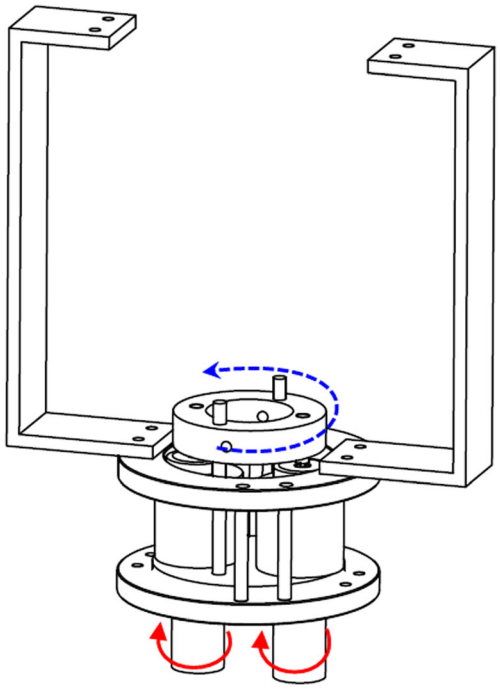

Fig. 4 Schematic diagram of planetary motion mechanism

seen, the PM-2DVMAF control system is composed of the programmable logic controller (PLC), motor drivers, and servomotors. Motor drivers receive digital signals sent by the PLC to drive the servomotors for different adjustments and controls so as to ensure that machining is conducted under the same conditions. Servo motor A is for adjusting the rotational speed of planetary motion (range, 100–1,000 rpm); servomotor B, for adjusting the rotational speed of eccentric sleeve so as to control the frequency of vibration of workpiece (range, 0–16.67 Hz); servomotor C, for adjusting the working gap (range, 0.5–2 mm); and servomotor D, for controlling the position of the workpiece.

2.2 Vibration assistance mechanism

Figure 2 shows the exploded view of the vibration assistance mechanism. As can be seen, the magnet and workpiece platform is connected by a bearing to the eccentric sleeve, which vibrates at a 0.1–0.9-mm amplitude when driven by a servomotor. The magnet and workpiece platform is supported by two plastic impact dampers, one on each side. These dampers provide a cushioning effect to prevent rotation of workpiece under vibration along the *X*- and *Y*-directions.

2.3 Planetary motion

Figure 3 shows the exploded view of the planetary motion mechanism. As can be seen, the mechanism comprises an internal gear and two spur gears. With the internal gear being fixed, the spindle motor will drive coupling A, which is connected to the spur gear by the bearing shaft and bearing. Thus, coupling A in motion will cause the spur gears to both rotate and revolve. Coupling B connects the spur gears to the turntable and the magnets. The magnetic field generated will gather the non-sintered magnetic abrasives comprising steel particles mixed with SiC to form a flexible magnetic brush. To ensure steady rotation, the magnets should be kept perpendicular to the workpiece. As mentioned above, driven by a servomotor, the magnet and workpiece platform are vibrated along the *X*- and *Y*-directions at a 0.1–0.9-mm amplitude to perform surface polishing. Figure 4 is a schematic diagram of the planetary motion mechanism.

2.4 Motions and polishing paths of PM-2DVAMAF and MAF

Figure 5 illustrates the polishing motion of PM-2DVAMAF and MAF. As seen in Fig. 5a, the spindle motor turns anticlockwise (blue arrow) to drive the coupling, causing the magnets to revolve in the same anticlockwise direction as the spindle motor. Simultaneously, the relative motion of the internal gear and spur gears also causes the magnets to rotate clockwise (green arrow). As a result, surface finishing will proceed with the abrasive in both rotation and revolution. Comparatively, traditional MAF involves only rotation of the magnet and the abrasive.

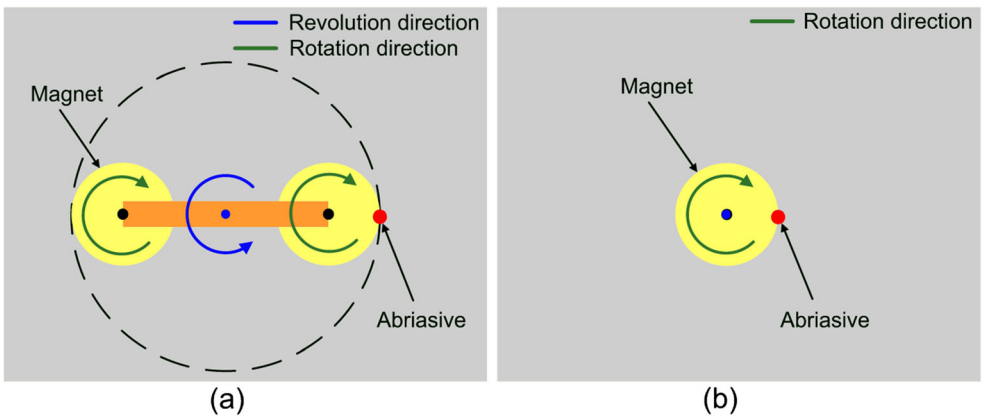

Fig. 5 Polishing motion of **a** PM-2DVAMAF and **b** MAF

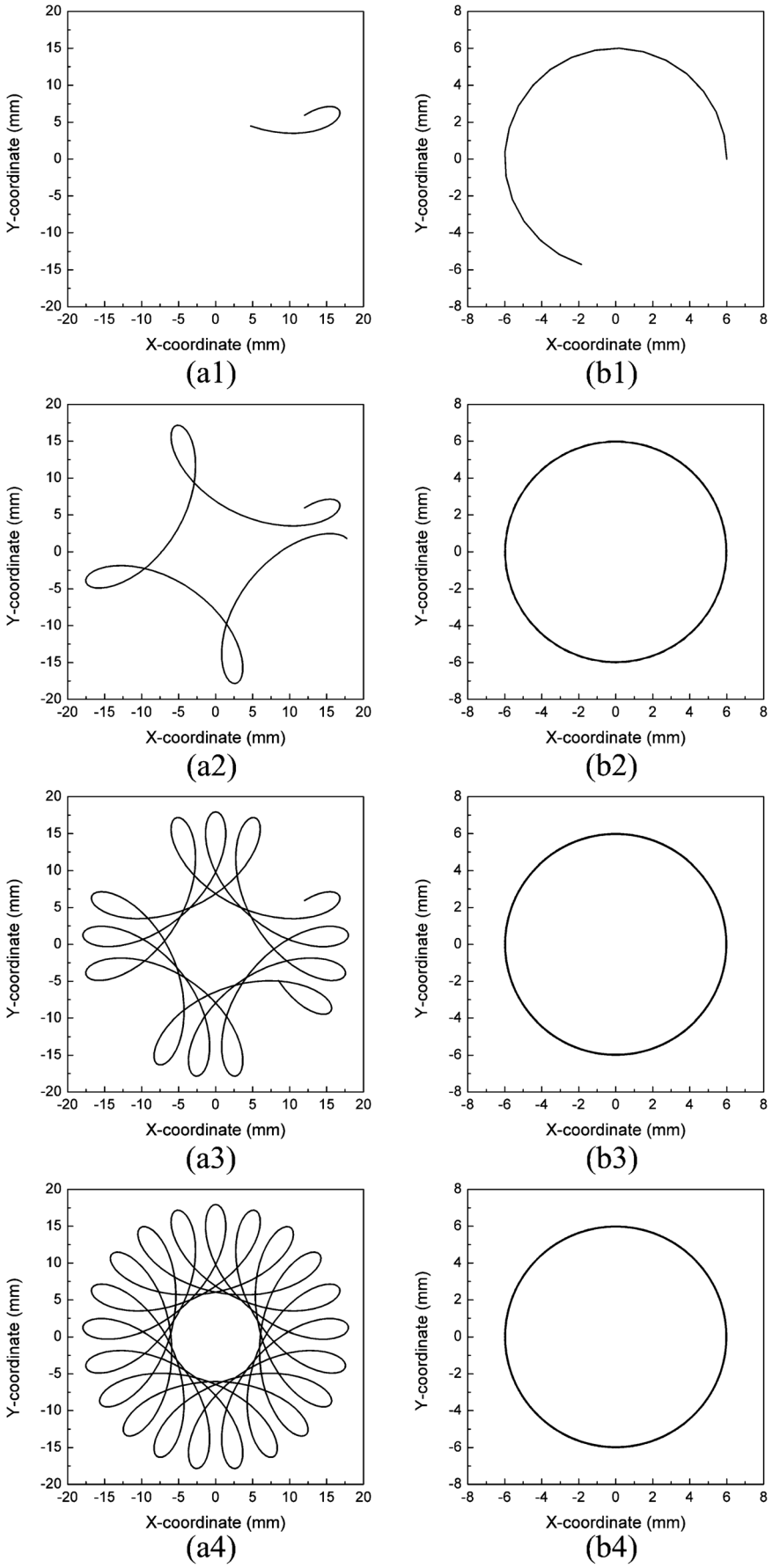

Fig. 6 Polishing paths under PM-2DVAMAF and MAF

Table 1 Chemical composition of SUS304 stainless steel

	C	Si	Mn	P	S	Ni	Cr
Chemical composition (wt%)	≤0.08	≤1.0	≤2.0	≤0.035	≤0.03	8.0–10.5	18.0–20.0

The polishing paths of a single abrasive under PM-2DVAMAF and MAF at a rotational speed of 500 rpm and machining time of 2.5 s are shown in Fig. 6. As can be seen, there are significant differences. The polishing path of MAF, as shown in Fig. 6(b1–b4) is a single circle whose diameter corresponds with that of the magnet. In contrast, the polishing paths under planetary motion of the internal gear and spur gears are intersecting and more closely packed, which can achieve better surface finishing.

In summary, planetary motion combined with 2D VAMAF causes abrasives to rotate and revolve. Not only can PM-2DVAMAF enhance material removal on the workpiece surface, it can also achieve more efficient deburring. The intersecting and closely packed polishing paths contribute to produce better surface quality.

2.5 Materials and methods

The 100×64×2-mm^3 workpiece is made of SUS304 stainless steel. It is manufactured first by hot rolling, followed by cold rolling, and finally processed into a flat surface. Table 1 shows the chemical composition of SUS304 stainless steel. The machining tool of 12-mm diameter and 50-mm length is made of N35 Nd-Fe-B magnet.

Table 2 displays the experimental parameters and levels for PM-2DVAMAF. These parameters are chosen with reference to the optimal settings obtained in our earlier research on 2D VAMAF [8]. The parameter levels in [8] are adopted as the median value in this experiment for more refined investigation.

Prior to the experiment, the SiC abrasives and the magnetic steel particles are weighed with a high-precision electronic balance and then mixed together with the machining fluid SAE40. The workpiece is first washed in an ultrasonic cleaner for 20 min before being placed onto the PM-2DVAMAF platform for machining. After 12.5-min processing, the workpiece is again washed in an ultrasonic cleaner for 20 min. Its surface morphology is then examined under a scanning electron microscope (SEM) (Hitachi S3500N) and its surface roughness is determined using a surface roughness measurement instrument (Kosaka Laboratory SEF-3500). Figure 7 illustrates the area machined and the region observed. Four observations are made on each workpiece specimen with each observation made after rotating counterclockwise the workpiece specimen at 90°.

3 Results and discussion

3.1 Optimal combination of PM-2DVAMAF parameters

3.1.1 Taguchi's orthogonal experiment

Table 3 lists the combination of factors in the L18 ($2^1\times3^7$) orthogonal array established using the Taguchi experimental design method [15–19] and the surface roughness obtained for each combination of parameters. All the experiments were conducted in triplicate for 12.5 min as per condition given in the table. Analysis of variance (ANOVA) was employed to assess the significant machining parameters affecting the surface quality. The optimal combination of parameters derived from the Taguchi experimental design and ANOVA was subject to reproducibility analysis. Experimental findings were

Table 2 Experimental parameters and levels for PM-2DVAMAF

Factors	Level 1	Level 2	Level 3
(A) Working gap (mm)	1	1.5	
(B) Amplitude of vibration (mm)	0.1	0.5	3
(C) Particle size of steel grit (mm)	0.3	0.18	0.125
(D) Weight of SiC (g)	2	3	4
(E) Weight of steel particles (g)	0.3	0.4	0.5
(F) Weight of machining fluid (g)	1	3	5
(G) Frequency of vibration (Hz)	8.33	16.67	25
(H) Rotational speed of magnet	300	500	700

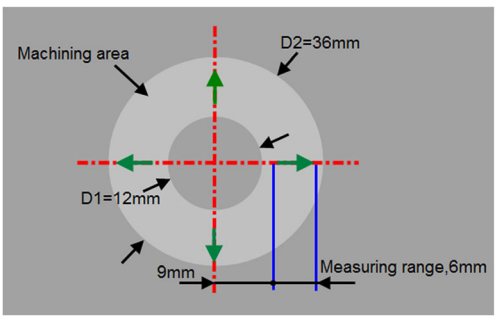

Fig. 7 Machined area and observed region on workpiece

Table 3 Design of experimental matrix and results

Exp	Factors								Surface roughness	
	A	B	C	D	E	F	G	H	Ra (μ)	S/N ratio (dB)
1	1	0.1	0.30	2	0.3	1	8.33	300	0.086	21.130
2	1	0.1	0.18	3	0.4	3	16.67	500	0.045	26.936
3	1	0.1	0.125	4	0.5	5	25	700	0.036	28.874
4	1	0.5	0.30	2	0.4	3	25	700	0.081	21.830
5	1	0.5	0.18	3	0.5	5	8.33	300	0.039	28.179
6	1	0.5	0.125	4	0.3	1	16.67	500	0.059	24.583
7	1	0.9	0.30	3	0.3	5	16.67	700	0.064	23.876
8	1	0.9	0.18	4	0.4	1	25	300	0.116	18.711
9	1	0.9	0.125	2	0.5	3	8.33	500	0.038	28.404
10	1.5	0.1	0.30	4	0.5	3	16.67	300	0.061	24.293
11	1.5	0.1	0.18	2	0.3	5	25	500	0.052	25.680
12	1.5	0.1	0.125	3	0.4	1	8.33	700	0.070	23.098
13	1.5	0.5	0.30	3	0.5	1	25	500	0.076	22.384
14	1.5	0.5	0.18	4	0.3	3	8.33	700	0.061	24.293
15	1.5	0.5	0.125	2	0.4	5	16.67	300	0.052	25.680
16	1.5	0.9	0.30	4	0.4	5	8.33	500	0.081	21.830
17	1.5	0.9	0.18	2	0.5	1	16.67	700	0.056	25.036
18	1.5	0.9	0.125	3	0.3	3	25	300	0.064	23.876

compared with the predicted results to validate the optimal combination of parameters.

Figure 8 shows the effect of different combinations of parameters on polishing performance denoted by the signal-to-noise (*S*/*N*) ratio. In this work, the predicted value of surface roughness should be "the lower the better" (LB). The *S*/*N* ratio, in unit of decibels, is calculated using the following equations:

$$\mathrm{LB}: \eta = -10\log\left[\frac{1}{n}\sum_{i=1}^{n} yi^2\right] \tag{1}$$

where *yi* denotes the experimental values of the *i*th experiment and *n* denotes the number of experiments performed.

$$\left[\frac{S}{N}\right]_{\text{prdicted}} = \left[\frac{S}{N}\right]_{\text{m}} + \sum_{i=1}^{n}\left(\left[\frac{S}{N}\right]_{i} - \left[\frac{S}{N}\right]_{\text{m}}\right) \tag{2}$$

where $[S/N]_{\text{predicted}}$ is the predicted *S*/*N* ratio, $[S/N]_{\text{m}}$ is the mean of all 18 *S*/*N* ratios obtained and $[S/N]_i$ is the *S*/*N* ratio of the *i*th experiment. The predicted surface roughness obtained

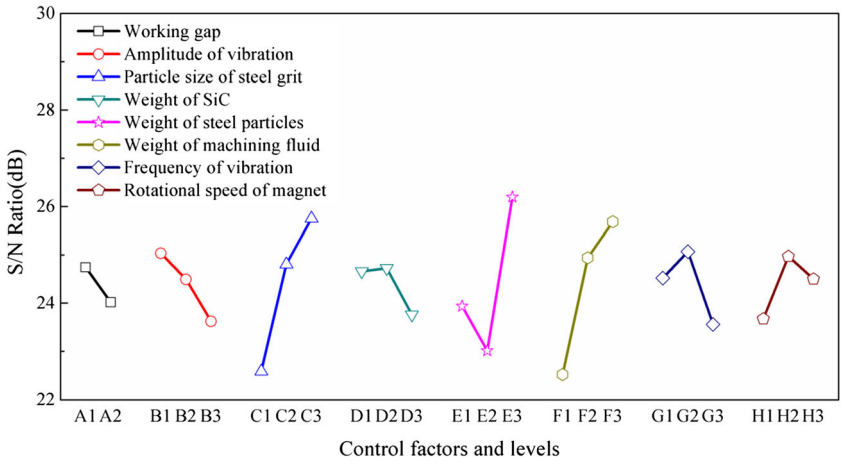

Fig. 8 Effect of polishing parameters on surface quality

Table 4 ANOVA and *F* test results

Factors	DOF	Sum of squares	Mean square	*F* value
A	(1)	2.370		
B	2	6.068	3.304	0.864
C	2	31.673	15.837	4.510[a]
D	(2)	3.499		
E	2	32.139	16.070	4.576[a]
F	2	32.867	16.434	4.680[a]
G	2	6.944	3.497	0.996
H	2	5.517	2.578	0.734
A×B	(2)	1.204		
Error	5	9.642	3.512	
Total	17	121.921		

[a] Significant factors [$F0.1(1,6)=3.78$, $F0.1(2,6)=3.46$]

using the optimal combination of parameters can be calculated using Eqs. 1 and 2.

According to the results shown in Fig. 8, the optimal combination of parameters should be A1B1C3D2E3F3G2H2, that is, working gap, 1 mm; amplitude of vibration, 0.1 mm; particle size of steel grit, 0.125 mm; weight of SiC, 3 g; weight of steel particles, 0.5 g; weight of machining fluid, 5 g; frequency of vibration along the *X*- and *Y*-directions, 16.67 Hz; and rotational speed of magnet, 500 rpm.

3.1.2 ANOVA and *F* test results

Table 4 lists the ANOVA results of surface roughness and Table 5 is the response table of the Taguchi experimental control factors for PM-2DVAMAF. As can be seen, the greater the effect of the parameter on surface roughness, the higher is its rank as a controlling factor. The parameters in order of their effect are weight of steel particles>weight of machining fluid>particle size of steel grit>frequency of vibration>amplitude of vibration>rotational speed of magnet>weight of SiC>working gap. Among them, weight of steel particles, weight of machining fluid, and particle size of steel grit have the greatest effect on surface quality attained by PM-2DVAMAF.

Table 6 Calculated and experimental results of optimal combination of parameters

Trial no.	Surface roughness Ra (μm)	
	Calculated	Experimental
1	0.027	0.032
2	0.027	0.032
3	0.027	0.032

3.1.3 Confirmation experiment

Reproducibility analysis was then performed to verify the optimal values of parameters derived from the Taguchi method and ANOVA. Table 6 compares the calculated and experimental results obtained by the optimal combination of parameters. As can be seen, in all three trials, the same results are obtained with the calculated values close to the actual surface roughness measured, indicating reliability of the Taguchi design method.

Figure 9 shows the three-dimensional surface profiles of workpiece surface before and after 12.5-min polishing by PM-2DVAMAF. As can be seen, surface roughness is greatly improved after polishing by PM-2DVAMAF under the optimal combination of parameters. The SEM image shown in Fig. 10 echoes the finding of enhanced surface quality achieved by PM-2DVAMAF.

3.2 Comparison of surface quality

Figure 11 plots the changes in surface roughness with processing time of MAF, 2D VAMAF, and PM-2DVAMAF. For the initial 50 s, measurement is taken every 10 s and thereafter at an interval of 60 s. As can be seen, surface roughness decreases with processing time with a more marked decline within the

Table 5 Response table of Taguchi experimental control factors for PM-2DVAMAF

Factors	Level 1	Level 2	Level 3	Effect	Rank	Optimal parameters
(A) Working gap (mm)	24.745	24.019		0.726	8	A1
(B) Amplitude of vibration (mm)	25.032	24.492	23.622	1.409	5	B1
(C) Particle size of steel grit (mm)	22.587	24.806	25.753	3.165	3	C3
(D) Weight of SiC (g)	24.657	24.725	23.764	0.961	7	D2
(E) Weight of steel particles (g)	23.937	23.014	26.195	3.181	1	E3
(F) Weight of machining fluid (g)	22.520	24.939	25.687	3.167	2	F3
(G) Frequency of vibration (Hz)	24.519	25.067	23.559	1.508	4	G2
(H) Rotational speed of magnet (rpm)	23.675	24.969	24.501	1.295	6	H2

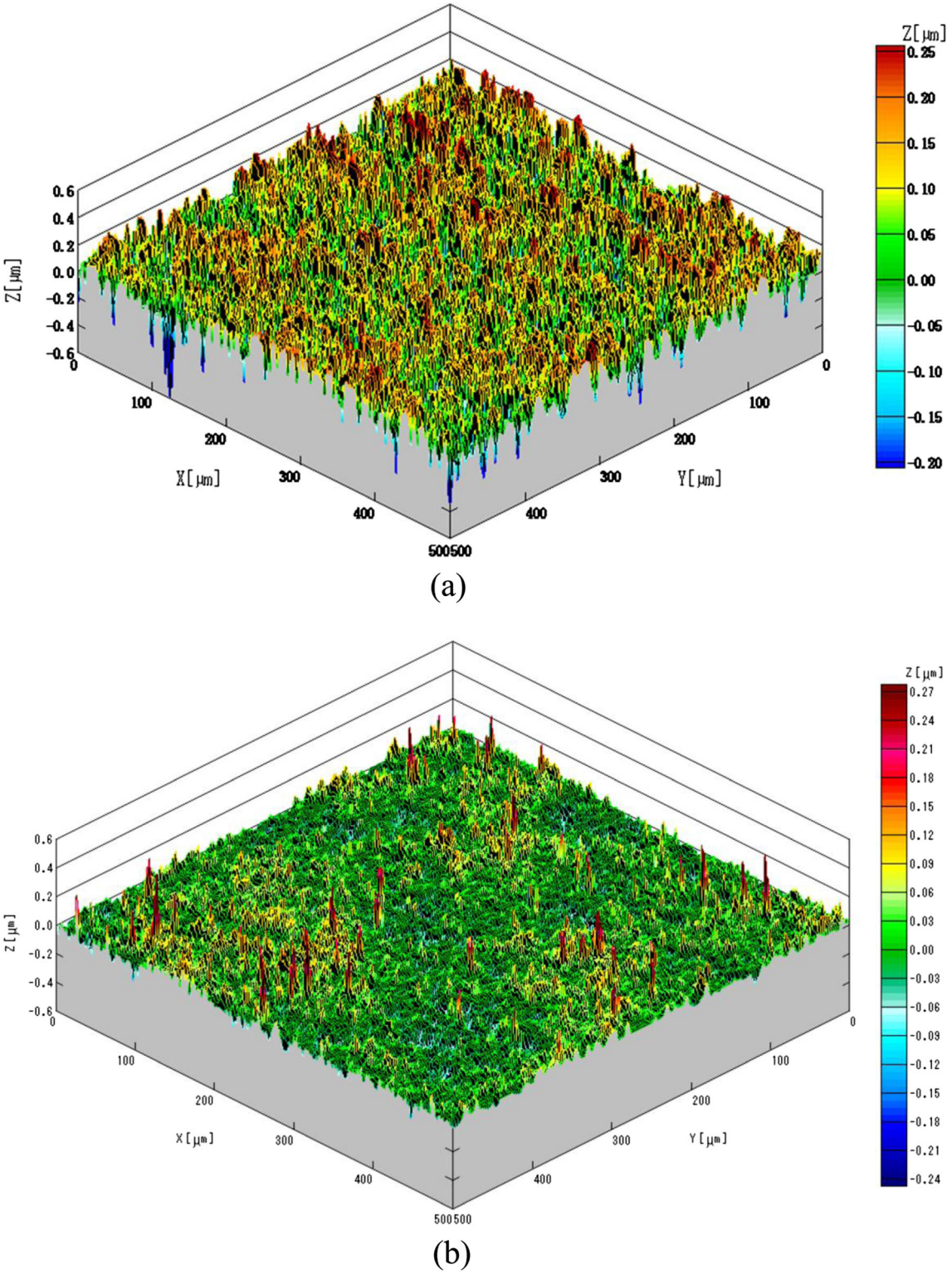

Fig. 9 Three-dimensional surface profiles of workpiece surface **a** before and **b** after PM-2DVAMAF

first minute. In addition, regardless of the processing time, PM-2DVAMAF yields the best surface roughness compared with 2D VAMAF and MAF, and the difference in Ra value increases with processing time. The reduction in Ra attained by PM-2DVAMAF, 2D VAMAF, and MAF after 5-min processing was from 0.14 μm to 0.048, 0.058, and 0.073 μm, indicating improvement of 65.7, 58.5, and 47.8 %, respectively. These results evidenced the superior machining efficiency of PM-2DVAMAF, which can contribute to shorter processing time required and, hence, low production cost.

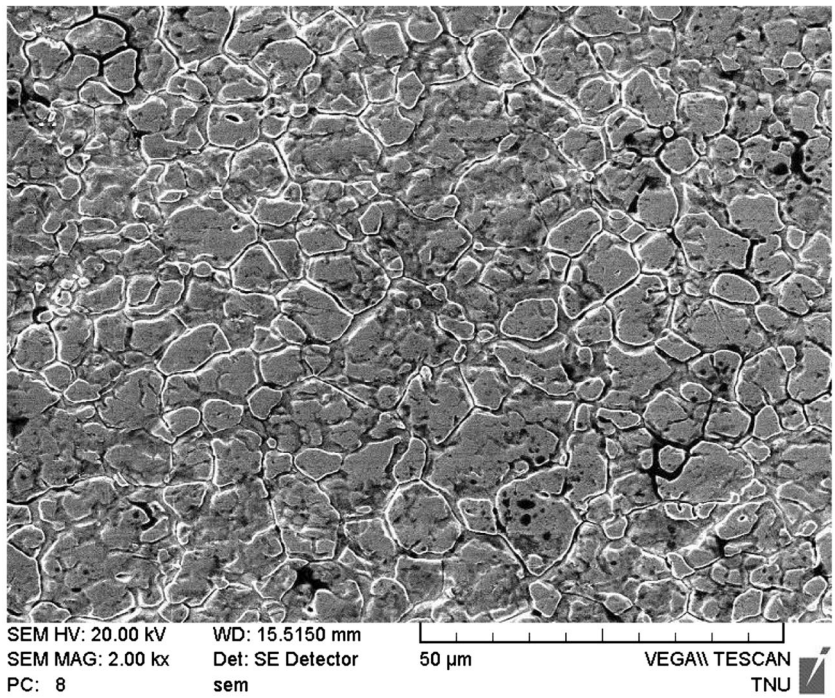

(a)

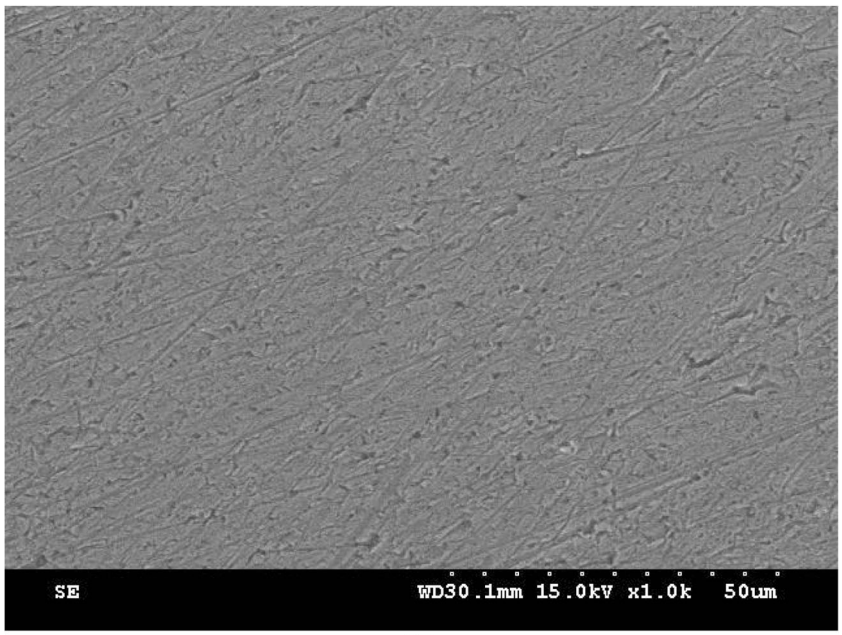

(b)

Fig. 10 SEM image of surface **a** before and **b** after PM-2DVAMAF

3.3 Effect of significant machining parameters on surface roughness

3.3.1 Weight of machining fluid

Figure 12 displays the changes in surface roughness with weight of machining fluid. As can be seen, the best surface quality (Ra=0.032 μm) is achieved using 5 g of machining fluid. The ANOVA results have shown that weight of machining fluid, which determines the concentration of SiC abrasives, is the key to enhancement in surface quality attained by PM-2DVAMAF. In other words, the ratio between weight of machining fluid and amount of SiC used would influence the cutting power of abrasives. As seen in the figure, adding 5 g of machining fluid to 3 g of SiC can reduce the Ra from 0.14 to 0.032 μm, showing an improvement rate of 77.1 %. When using machining fluid of <5 g in weight, the concentration of SiC becomes lower, thus weakening the

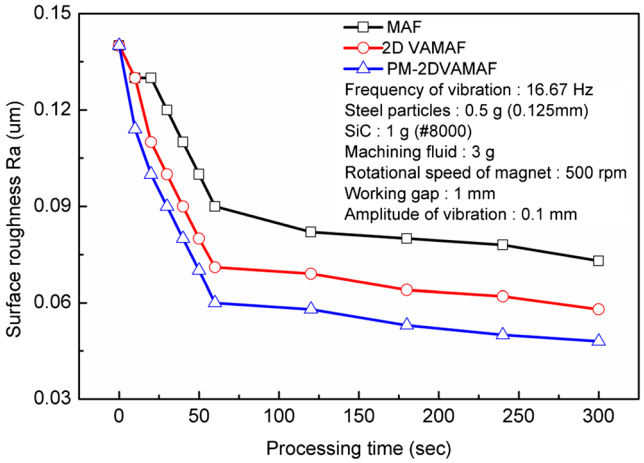

Fig. 11 Changes in surface roughness with processing time

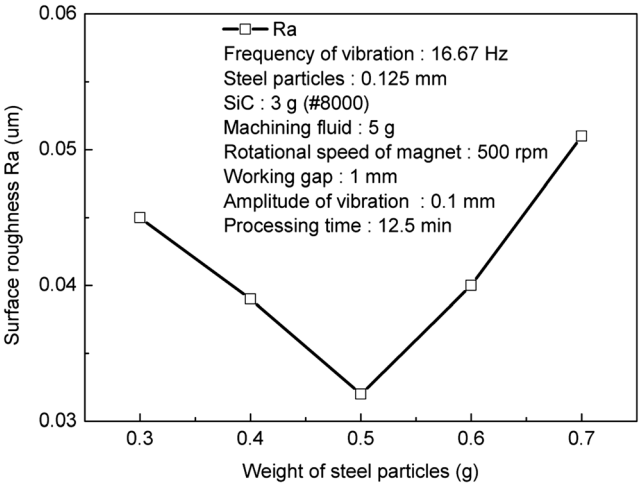

Fig. 13 Changes in surface roughness with weight of steel particles

cutting power of abrasives and leading to a smaller improvement in Ra. On the other hand, when using machining fluid of >5 g in weight, the concentration of SiC becomes higher and denser, thus also deteriorating the machining efficiency of abrasives with their motion and sliding being undermined. Hence, adding 7 g of machining fluid to 3 g of SiC can only reduce the Ra from 0.14 to 0.044 μm, showing an improvement rate of 68.5 % only.

3.3.2 Weight of steel particles

Figure 13 displays the changes in surface roughness with weight of steel particles. As can be seen, the best surface quality (Ra=0.032 μm) is achieved using 0.5 g of steel particles. Weight of steel particles has a direct influence on the strength of normal force exerted on the workpiece surface, under which polishing is performed by SiC abrasives. As shown in the figure, using 0.5 g of steel particles can reduce the Ra from 0.14 to 0.032 μm, showing an improvement rate of 77.1 %. In contrast, when using steel particles of <0.5 g in weight, the normal force exerted on the workpiece surface becomes lower in strength, thus weakening the machining power of abrasives and resulting in a smaller reduction in Ra. On the other hand, when using steel particles of >0.5 g in weight, undue normal force would be exerted, causing excessive machining and resulting in scratches formed on the workpiece surface. For example, using 0.7 g of steel particles would a high surface roughness of 0.051 μm.

3.3.3 Particle size of steel grit

Figure 14 plots the changes in surface roughness with particle size of steel grit. As can be seen, there exists a linear relationship between the two, that is, the larger the particle size of steel grit, the higher is the surface roughness. The uneven edges of the steel grit will form scratches on the workpiece surface; hence, larger steel particles will form wider and deeper scratches. In addition, smaller steel particles which can be

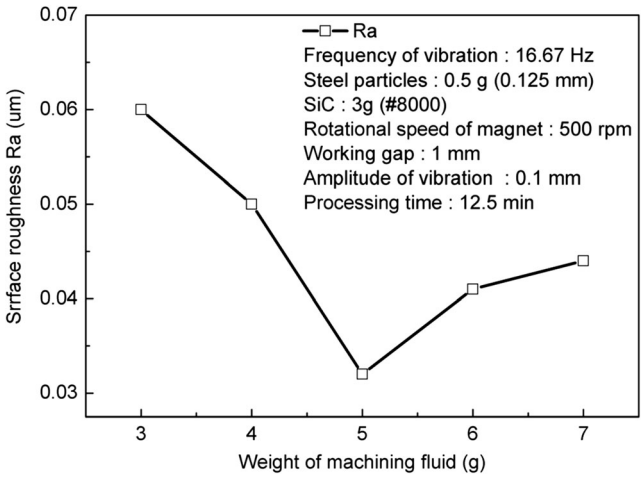

Fig. 12 Changes in surface roughness with weight of machining fluid

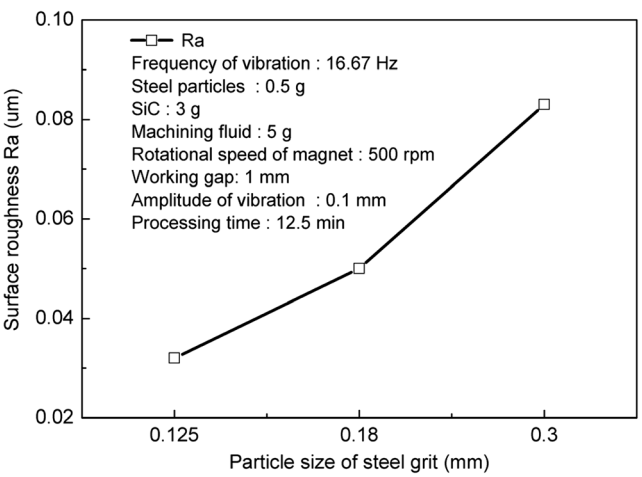

Fig. 14 Changes in surface roughness with particle size of steel grit

packed more closely and densely would exert more uniform normal force on the workpiece surface. The results evidence that the lowest surface roughness of 0.032 μm is attained by steel particle of size 0.125 mm, an improvement rate of 77.1 %, compared with that of 0.083 μm attained by larger steel particle of size 0.3 mm.

3.3.4 Frequency of vibration

Figure 15 shows the changes in surface roughness with frequency of vibration. As can be seen, the best surface quality (Ra=0.032 μm) is achieved using a vibration frequency of 16.67 Hz. Surface roughness decreases from the initial Ra of 0.059 μm obtained by PM with increasing frequency of vibration and reaches the lowest of 0.032 μm at 16.67 Hz, an improvement rate of 77.1 %. The results evidence better polishing performance and better surface roughness under vibration assistance and planetary motion. The improvement in surface quality is attributed to the enhanced machining power of abrasives under vibration, rotation, and revolution, all of which contribute to intersecting and closely packed polishing paths, as shown in Fig. 6. However, vibration frequency exceeding 16.67 Hz deteriorates, rather than improves, surface roughness, as evidenced by Ra of 0.043 μm attained at a vibration frequency of 25 Hz, compared with that at 16.67 Hz.

3.3.5 Amplitude of vibration

Figure 16 plots the changes in surface roughness with amplitude of vibration. As can be seen, there exists a linear relationship between the two, that is, the larger the amplitude of vibration, the higher is the surface roughness. As shown in the experimental setup, the magnet and workpiece platform is connected to the eccentric sleeve for motion; hence, both frequency and amplitude of vibration would affect the polishing performance. The results show that the lowest surface roughness of 0.032 μm is attained at a vibration amplitude of 0.1 mm. It is because a small amplitude of vibration would imply more even machining with more uniform and denser polishing paths formed while a large amplitude of vibration causes violent shaking, resulting in poorer polishing performance.

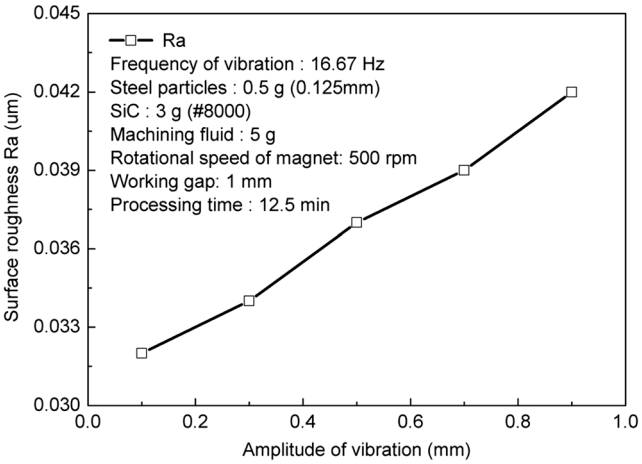

Fig. 16 Changes in surface roughness with amplitude of vibration

3.3.6 Rotational speed of magnet

Figure 17 shows the changes in surface roughness with rotational speed of magnet. As can be seen, the best surface quality (Ra=0.032 μm) is achieved at a rotational speed of magnet of 500 rpm. At low rotational speed <500 rpm, the relative motion between abrasives and workpiece is kept so low that there is limited abrasion, while at high rotational speed >500 rpm, the abrasives will be dispersed from the working gap, which would in turn deteriorate polishing performance. Moreover, high rotational speed would also cause excessive machining, resulting in poorer surface quality.

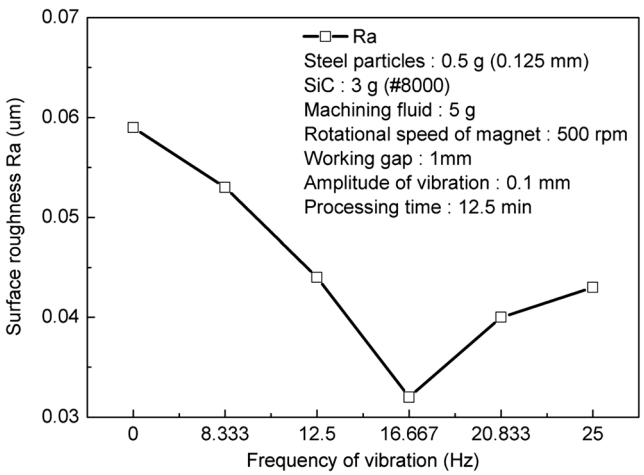

Fig. 15 Changes in surface roughness with frequency of vibration

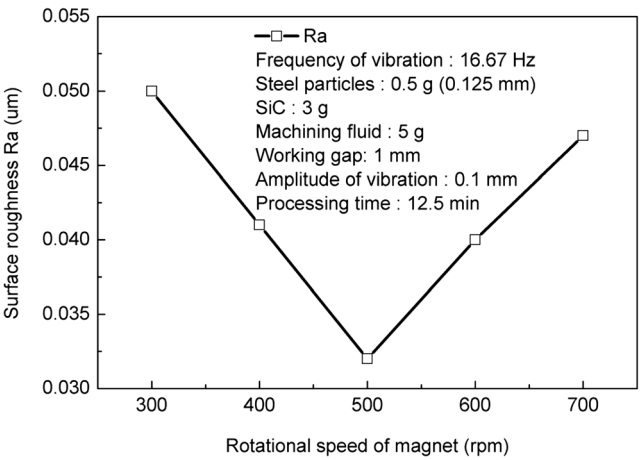

Fig. 17 Changes in surface roughness with rotational speed of magnet

4 Conclusions

This study explores the effects of combining PM with two-dimensional vibration-assisted MAF for enhancing polishing performance and improving surface quality. The following conclusions are drawn from the experimental results.

1. The polishing path of MAF is a single circle whose diameter corresponds with that of the magnet. In contrast, the polishing paths under PM are intersecting and more closely packed. PM-2DVAMAF also causes abrasives to rotate and revolve along the intricate and extensive polishing paths, thus contributing to better surface quality.
2. Obtained by the Taguchi experimental design, the optimal combination of parameters for improving surface roughness includes working gap, 1 mm; amplitude of vibration, 0.1 mm; particle size of steel grit, 0.125 mm; weight of SiC, 3 g; weight of steel particles, 0.5 g; weight of machining fluid, 5 g; frequency of vibration along the *X*- and *Y*-directions, 16.67 Hz; and rotational speed of magnet, 500 rpm.
3. With 12.5-min PM-2DVAMAF under optimal combination of parameters, the surface roughness of a stainless steel SUS304 workpiece can be reduced from 0.14 to 0.032 μm, an improvement rate of 77.1 %.
4. Three-dimensional profiles of finished surface evidence the efficient removal of scratches under PM-2DVAMAF and further enhancement in surface quality.
5. Experimental results show that PM-2DVAMAF is superior to traditional MAF and 2D VAMAF. Not only can it improve surface quality, a shorter processing time and a smaller amount of abrasives are required, both of which contribute to cost reduction.

References

1. Mulik RS, Pandey PM (2011) Magnetic abrasive finishing of hardened AISI 52100 steel. Int J Adv Manuf Technol 55(5–8):501–515
2. Amineh SK, Tehrani AF, Mohammadi M (2013) Improving the surface quality in wire electrical discharge machined specimens by removing the recast layer using magnetic abrasive finishing method. Int J Adv Manuf Technol 66(9–12):1793–1803
3. Givi M, Tehrani AF, Mohammadi A (2012) Polishing of the aluminum sheets with magnetic abrasive finishing method. Int J Adv Manuf Technol 61(9–12):989–998
4. Liu ZQ, Chen Y, Li YJ, Zhang X (2013) Comprehensive performance evaluation of the magnetic abrasive particles. Int J Adv Manuf Technol. doi:10.1007/s00170-013-4783-6
5. Shinmura T, Takazawa K, Hatano E (1986) Study on magnetic abrasive finishing (1st report): process principle and a few finishing characteristics. J Jpn Soc Precis Eng 52:851–857
6. Shinmura T, Hatano E, Takazawa K (1986) Development of plane magnetic abrasive finishing apparatus and its finishing performance. J Jpn Soc Precis Eng 52:1080–1086
7. Kim JD, Choi MS (1997) Study on magnetic polishing of free-form surface. Int J Mach Tool Manuf 37:1179–1187
8. Lee YH, Wu KL, Bai CT, Liao CY, Yan BH (2013) Two-dimensional vibration-assisted magnetic abrasive finishing of stainless steel SUS304. Int J Adv Manuf Technol 69:2723–2733
9. Mulik RS, Pandey PM (2010) Mechanism of surface finish in ultrasonic-assisted magnetic abrasive finishing process. Mater Manuf Process 25:1418–1427
10. Mulik RS, Pandey PM (2011) Ultrasonic assisted magnetic abrasive finishing of hardened AISI 52100 steel using unbonded SiC abrasives. Int J Refract Met Hard Mater 29:68–77
11. Yin S, Shinmura T (2004) Vertical vibration-assisted magnetic abrasive finishing and deburring for magnesium alloy. Int J Mach Tools Manuf 44:1297–1303
12. Wang Y, Hu D (2005) Study on the inner surface finishing of tubing by magnetic abrasive finishing. Int J Mach Tools Manuf 145:43–49
13. Jain VK, Kumar P, Behera PK, Jayswal SC (2001) Effect of working gap and circumferential speed on the performance of magnetic abrasive finishing process. Wear 250:384–390
14. Hung CL, Ku WL, Yang LD (2010) Prediction system of magnetic abrasive finishing (MAF) on the internal surface of cylindrical tube. Mater Manuf Process 25:1404–1412
15. Singh S, Shan HS, Kumar P (2002) Parametric optimization of magnetic-field-assisted abrasive flow machining by the Taguchi method. Qual Reliab Eng Int 18:273–283
16. Liao HT, Shie JR, Yang YK (2008) Applications of Taguchi and design of experiments methods in optimization of chemical mechanical polishing process parameters. Int J Adv Manuf Technol 38:674–682
17. Yang LD, Lin CT, Chow HM (2009) Optimization in MAF operations using Taguchi parameter design for AISI304 stainless steel. Int J Adv Manuf Technol 42(5–6):595–605
18. Mali HS, Manna A (2012) Simulation of surface generated during abrasive flow finishing of Al/SiCp-MMC using neural networks. Int J Adv Manuf Technol 61:1263–1268
19. Prabhu S, Vinayagam B (2012) AFM investigation in grinding process with nanofluids using Taguchi analysis. Int J Adv Manuf Technol 60:149–160